# SNP rs4142441 and MYC co-modulated long non-coding RNA OSER1-AS1 suppresses non-small cell lung cancer by sequestering RNA-Binding Protein ELAVL1

**Weijia Xie**
Army Medical University
**Youhao Wang**
Army Medical University
**Yao Zhang**
Army Medical University
**Ying Xiang**
Army Medical University
**Na Wu**
Army Medical University
**Long Wu**
Army Medical University
**Chengying Li**
Army Medical University
**Tongjian Cai**
Army Medical University
**Xiangyu Ma**
Army Medical University
**Zubin Yu**
Army Medical University
**Li Bai**
Army Medical University
**Yafei Li** ( liyafei2008@tmmu.edu.cn )

---

**Research**

**Keywords:** Long non-coding RNA, OSER1-AS1, non-small cell lung cancer, miR-17-5p, ELAVL1

**Posted Date:** May 22nd, 2020

**DOI:** https://doi.org/10.21203/rs.3.rs-30031/v1

# Abstract

**Background**: Single nucleotide polymorphisms (SNPs) and long non-coding RNAs (lncRNAs) have been involved in the process of lung cancer. Following clues given by lung cancer risk-associated SNPs, we aimed to find novel functional lncRNAs as candidate targets in non-small cell lung cancer (NSCLC).

**Methods**: Case-control analyses were performed in 626 cases and 736 controls matched up on sex and age. The lncRNA OSER1-AS1 was identified near a lung cancer risk-associated SNP rs4142441. Kaplan–Meier survival analysis was performed to investigate the association between OSER1-AS1 expression and overall survival. The influence of rs4142441 on the expression level of OSER1-AS1 was confirmed using Luciferase assays. Subsequently, the biological function of OSER1-AS1 was assessed *in vitro* by cell proliferation, migration, and invasion experiments through gain- and loss-of-function approaches, and *in vivo* by subcutaneous tumor model and tail vein injection lung metastasis model. ChIP and RIP experiments were carried out to investigate the interaction between transcription factors, RNA-binding proteins, and OSER1-AS1.

**Results**: OSER1-AS1 was down-regulated in tumor tissue and its low expression was significantly associated with poor overall survival among non-smokers in NSCLC patients. Gain- and loss-of-function studies revealed that OSER1-AS1 acted as a tumor suppressor by inhibiting lung cancer cell growth, migration and invasion *in vitro*. Xenograft tumor assays and metastasis mouse model confirmed that OSER1-AS1 suppressed tumor growth and metastasis *in vivo*. The promoter of OSER1-AS1 was repressed by MYC, and the 3’-end of OSER1-AS1 was competitively targeted by microRNA hsa-miR-17-5p and RNA-binding protein ELAVL1.

**Conclusion**: Our results indicated that OSER1-AS1 exerted tumor-suppressive functions by acting as an ELAVL1 decoy to keep it away from its target mRNAs. Our findings characterized OSER1-AS1 as a new tumor suppressive lncRNA in NSCLC, suggesting that OSER1-AS1 may be suitable as a potential biomarker for prognosis, and a potential target for treatment.


# Background

Lung cancer is one of the leading causes of cancer-associated deaths worldwide [1]. The 5-year survival rate was only 15% during the past few decades [2]. Non-small cell lung cancer (NSCLC) accounts for 85% of all lung cancer cases [3, 4].

Long noncoding RNAs (lncRNAs) are a new class of potential biomarkers and therapeutic targets for lung cancer. So far, studies have identified various lncRNAs that contribute to cancerous phenotypes such as proliferation, growth suppression, motility, immortality, and angiogenesis in lung cancer [5–10]. On the other hand, numerous single nucleotide polymorphisms (SNPs) have been associated with lung cancer risks in the past decade [11]. Some of these SNPs are located near lncRNAs and they may help to highlight the potential lung cancer-related lncRNAs in its vicinity.

In this study, we first performed case-control studies to identify SNPs associated with NSCLC risks. To increase the strength of evidence, we integrated information gathered from various bioinformatics platforms and examined the potential prognostic values of lncRNAs at these NSCLC-associated loci. Next, we performed functional studies to investigate the underlying molecular mechanisms of these lncRNAs. LncRNAs have been known to function primarily through their interaction with microRNAs, DNA, RNA or RNA-binding proteins via the competitive endogenous RNA network (ceRNA network)[12–14]. Therefore, we particularly focused on investigating the potential ceRNA interactions in the post-transcriptional gene regulation process.

We now show that a lncRNA OSER1-AS1, near the NSCLC-associated SNP rs4142441, was differentially expressed between lung cancer and adjacent normal tissues. We examined the effect of OSER1-AS1 knockdown and overexpression on cell proliferation, migration and invasion in NSCLC cells. We found that OSER1-AS1 was transcriptionally repressed by MYC at the promoter, and down-regulated by microRNA hsa-miR-17-5p at the 3'-end. Interestingly, OSER1-AS1 may function as a decoy for RNA-binding protein ELAV-like protein 1 (ELAVL1, or human antigen R (HuR)), which was one of the most widely studied regulators of cytoplasmic mRNA stability.

## Materials And Methods

# Selection of SNPs and genotyping

We selected 16 SNPs located near potential lung cancer-related lncRNAs following the procedure described in **Supplementary Fig. 1**. Additional details about the selecting procedure are available in the **Supplementary Methods**. The selected SNPs (**Supplementary Table S1)** were used for case-control analysis.

# Case-control analysis

New cases diagnosed with NSCLC were collected from Xinqiao Hospital of the Army Medical University (Third Military Medical University) in Chongqing, China. Healthy controls were collected from the annual physical examination group in the same hospital. Additional details about the inclusion/exclusion criteria for case and controls are described in the Supplementary Methods. We matched up 645 patients on age and sex with 748 healthy controls. Demographic and other risk information was obtained from subjects via a combination of a structured subject interview and medical records. Blood samples were collected from controls and patients prior to any treatment. All subjects provided informed written consent. Research protocol was approved by the ethics committee of the Army Medical University.

# Human tissue samples

Tissue specimens were collected from lung cancer patients prior to any radiation or chemotherapy during operation. The freshly frozen lung tumors and matched normal lung tissues were sectioned and reviewed by a pathologist to confirm the diagnosis of lung cancer, histological grade, tumor purity, and lack of

tumor contamination in the normal lung. Tumor samples with ≥ 70% tumor-cell content and matched normal lung tissues were used in the study.

# Cell culture and treatment

The lung cancer cell lines A549, SPCA1, and H1299 were obtained from the Cell Bank of the Chinese Academy of Science (Shanghai, China) and the American Type Culture Collection (ATCC, Manassas, VA, USA), cultured in RPMI-1640 (HyClone, Logan, UT, USA) supplemented with 10% fetal bovine serum (HyClone, Logan, UT, USA).

# qRT-PCR analysis

Total RNA was extracted using the TRIzol reagent (TaKaRa, Dalian, China). The cDNAs were amplified using PrimeScript™ RT reagent Kit with gDNA Eraser (TaKaRa). Real-time RT-PCR assay was performed using a SYBR PrimeScript RT-PCR Kit according to the standard manufacturer's instructions (TaKaRa, Dalian, China). Results were normalized to the housekeeping gene β-actin. The nuclear and cytoplasmic RNA were isolated using PARIS™ Kit (Invitrogen, NY, USA). Primers sequences were provided in **Supplementary Table S2**.

# RNA Fluorescence in situ hybridization

Cy3-labeled OSER1-AS1 probes were synthesized by GenePharma (Shanghai, China). RNA-FISH was performed as described by Zhou et al [15] following the manufacturer's instructions. U6 snRNA and 18S rRNA probes were purchased from GenePharma (Shanghai, China) and were used as nuclear and cytoplasmic localization control, respectively.

# Plasmid construction and cell transfection

To construct plasmids expressing OSER1-AS1, MYC and ELAVL1, the full-length human OSER1-AS1 sequence (Transcript ID: ENST00000442383.1), MYC(Transcript ID: ENST00000621592.7) and ELAVL1 (Transcript ID: ENST00000407627.7) were synthesized and subcloned into the pcDNA3.1 vector (Invitrogen, New York, USA). The stable transfected cells were selected under Geneticin (G418 sulfate) (Sangon, Shanghai, China). OSER1-AS1 siRNA sequences were shown in **Supplementary Table S2**. Hsa-miR-17-5p mimics, inhibitors, negative controls and inhibitor-controls were purchased from GenePharma (**Supplementary Table S2**). To avoid the interference of hsa-miR-17-5p (the reverse complementary sequence of hsa-miR-17-5p) [16], we used single strand hsa-miR-17-5p mimics for this study.

# Cell Counting Kit-8 assay, colony formation assay, cell migration and invasion assays *in vitro*

Cell Counting Kit-8 (CCK-8) assay, colony formation assay, cell migration and invasion assays were performed as described in Yuan et al., 2016.[17]

# Animal experiments *in vivo*

For in vivo tumorigenicity, ten male BALB/c-nude mice (4-week-old) were randomly divided into two groups, with five mice in each group. Stable transfected A549 cells ($5.0 \times 10^6$) were injected subcutaneously into the left flanks of the nude mice (100 ul per mouse). The tumor volume was calculated using the equation $V = 0.5 \times D \times d^2$ (V, volume; D, longitudinal diameter; d, latitudinal diameter). We observed the tumor growth for 5 weeks. For metastasis model, ten male BALB/c mice (4-week-old) were randomly divided into two groups, with five mice in each group. Stable transfected A549 cells ($1 \times 10^6$) were injected into their tail veins (100 ul per mouse). The mice were sacrificed 5 weeks after injection and the lungs were removed for further analysis. All experimental animal procedures were approved by the Institutional Animal Care and Use Committee of Third Military Medical University.

# Luciferase reporter assay

To evaluate the miRNA/ELAVL1-lncRNA interaction by luciferase reporter assay, the hsa-miR-17-5p binding sites of OSER1-AS1 3'-end region were inserted into the Pischeck-2 vector (Promega), and ELAVL1 was inserted into pcDNA3.1 vector (Sangon, Shanghai, China). Firefly and Renilla luciferase activities were measured 48 hours after transfection using the Dual-Luciferase Assay System (Promega). The relative luciferase activity was calculated using renilla/firefly luciferase activity.

To evaluate the binding of MYC to the promoter of OSER1-AS1, the OSER1-AS1 promoter sequence (-1000 bp ~ + 1000 bp) was synthesized and subcloned into the luciferase reporter vector pGL3-basic (Promega), for which two versions were constructed: WT with allele A for rs4142441 and MUT with allele G for rs4142441. The plasmids were co-transfected with pcDNA3.1-MYC as well as pRL-SV40 Renilla luciferase plasmid (Promega) for internal control.

# Western blot

Western blot (WB) was performed as described previously (Yuan et al., 2016) [17]. The antibodies used in this study were rabbit monoclonal to MYC (Abcam Inc., Cambridge, MA) (1:2000; Abcam (ab32072)), rabbit monoclonal to ELAVL1 (1:5000; Abcam (ab200342)), rabbit monoclonal to AGO2 (1:2000; Abcam (ab186733)), rabbit monoclonal to BCL2L11 (1:2000; Abcam (ab32158)), rabbit monoclonal to Histone H3 (1:5000; Abcam (ab176842)), rabbit polyclonal to β-actin (1:5000; Abcam (ab8227)). Immunohistochemistry was performed as described in Liu et al [18]. using the rabbit monoclonal to Ki-67 (1:500; Abcam).

# Chromatin immunoprecipitation assay

Chromatin immunoprecipitation (ChIP) assay was performed following the protocol of ChIP Assay Kit (Beyotime Institute of Biotechnology, Jiangsu, China). Briefly, crosslinked chromatin was prepared with 1% formaldehyde for 10 min at 37 °C and the DNA was shredded to an average length of 200–1000 bp by sonication. Immunoprecipitation were conducted using rabbit polyclonal to MYC (Abcam) or IgG

control. Precipitated DNA was amplified by PCR. Primers sequences are provided in **Supplementary Table S2**.

# RNA-binding protein immunoprecipitation assay

RNA-binding protein immunoprecipitation assay was performed following the protocol of Magna RIP™ RNA-Binding Protein Immunoprecipitation Kit (MilliporeSigma, US). The nuclear and cytoplasmic RNA was separated by using the Membrane, Nuclear and Cytoplasmic Protein Extraction kit (Sangon) with added RNase Inhibitor (Beyotime Institute of Biotechnology, Jiangsu, China) to a final concentration of 1 U/ul. After the lysate was prepared, 100 ul of whole/nuclear/cytoplasmic lysate were incubated at 4$^{o}$C overnight with 50 ul of magnetic beads pre-coated with 5ug ELAVL1 antibody or 5ug of AGO2 antibody. Another 100 ul aliquot of cell lysate was incubated with 50 ul of magnetic beads pre-coated with 5 ug of IgG antibody as a negative control.

# Bioinformatics analysis for TCGA-LUAD data

Additional descriptions of the bioinformatic analysis for TCGA-LUAD data are shown in the Supplementary Methods.

# Statistical analysis

We performed a multivariate logistic regression analysis on the association of SNPs with lung cancer by adjusting for age, sex, and smoking. Cell growth and migration results were evaluated using the two-tailed Student's *t*-test. Gene expression analyses were evaluated using the two-tailed Student's *t*-test or Mann-Whitney U-test. Pearson correlation was performed to analyze the correlation between miRNA and mRNA expressions. A two-sided P-value less than 0.05 was taken as statistically significant. Statistical analyses were performed using the software STATA version 12.0 (STATA Corp., Texas, USA). and software R (version 3.4.2).

## Results

# Rs4142441 associated with NSCLC risk in non-smokers is located in the promoter of OSER1-AS1

We performed case-control analysis for the 16 SNPs **(Supplementary Table S1)** selected through the bioinformatic pipeline as described in **Supplementary Figure S1** in 626 cases and 736 controls. Baseline characteristics of cases and controls were shown in **Supplementary Table S3**. We found no significant associations between any of the SNPs and lung cancer risks (Table 1). However, after stratifying by smoking status, we identified one significant association in the non-smoker group at rs4142441 in the promoter region of lncRNA OSER1-AS1 and lung cancer risk (OR = 1.712;95% CI:1.137–2.579， *P* = 0.01) (Table 1).

Table 1
The association between SNPs and lung cancer risks stratified by smoking status

| | | All (N = 1347)[1] | | Smoker (N = 735)[2] | | Non-smoker (N = 612) [3] | |
|---|---|---|---|---|---|---|---|
| SNPs | Effect allele/ other allele | OR (95% CI) | *P*-value | OR (95% CI) | *P*-value | OR (95% CI) | *P*-value |
| rs10134980 | C/A | 0.913 (0.75,1.111) | 0.362 | 0.84 (0.632,1.117) | 0.230 | 1.053 (0.767,1.446) | 0.751 |
| rs1059292 | T/C | 0.984 (0.786,1.232) | 0.889 | 1.178 (0.864,1.606) | 0.300 | 0.744 (0.514,1.076) | 0.116 |
| rs11655237 | C/T | 1.081 (0.894,1.307) | 0.422 | 1.153 (0.882,1.508) | 0.298 | 0.895 (0.659,1.216) | 0.479 |
| rs1549334 | G/A | 0.981 (0.816,1.179) | 0.837 | 1.089 (0.84,1.412) | 0.518 | 0.785 (0.575,1.072) | 0.128 |
| rs2239895 | G/C | 1.134 (0.904,1.423) | 0.276 | 1.064 (0.766,1.477) | 0.713 | 1.375 (0.951,1.987) | 0.090 |
| rs2275159 | G/A | 1.022 (0.845,1.236) | 0.821 | 1.111 (0.851,1.452) | 0.438 | 0.889 (0.655,1.207) | 0.450 |
| rs2295441 | T/C | 0.988 (0.842,1.159) | 0.880 | 0.981 (0.778,1.236) | 0.870 | 1.044 (0.808,1.351) | 0.741 |
| rs2302177 | T/G | 1.042 (0.889,1.221) | 0.613 | 1.098 (0.879,1.371) | 0.413 | 0.915 (0.703,1.191) | 0.511 |
| rs2720660 | G/A | 0.958 (0.74,1.241) | 0.745 | 0.969 (0.663,1.415) | 0.869 | 0.801 (0.537,1.194) | 0.275 |
| rs28631713 | G/A | 1.174 (0.949,1.452) | 0.140 | 1.098 (0.81,1.488) | 0.549 | 1.237 (0.884,1.732) | 0.215 |
| rs3093873 | T/C | 1.098 (0.893,1.351) | 0.375 | 1.118 (0.821,1.522) | 0.481 | 0.946 (0.686,1.304) | 0.733 |
| rs3200401 | T/C | 1.104 (0.882,1.38) | 0.388 | 0.903 (0.657,1.241) | 0.530 | 1.187 (0.835,1.687) | 0.340 |
| rs3783358 | G/C | 1.156 (0.978,1.367) | 0.089 | 1.187 (0.939,1.499) | 0.152 | 1.118 (0.85,1.471) | 0.425 |
| rs3788632 | T/C | 0.991 (0.787,1.248) | 0.937 | 1.131 (0.82,1.56) | 0.452 | 0.898 (0.604,1.337) | 0.597 |

1: Logistic regression adjusted for age, sex and smoking status (additive model)

2: Logistic regression adjusted for age and sex (additive model)

3: Logistic regression adjusted for age and sex (additive model)

| | | All (N = 1347)[1] | | Smoker (N = 735)[2] | | Non-smoker (N = 612) [3] | |
|---|---|---|---|---|---|---|---|
| rs3806357 | G/A | 0.964 (0.806,1.153) | 0.690 | 0.866 (0.671,1.117) | 0.267 | 1.153 (0.858,1.551) | 0.345 |
| rs4142441 | G/A | 1.178 (0.907,1.53) | 0.220 | 0.787 (0.543,1.141) | 0.206 | 1.712 (1.137,2.579) | **0.010*** |
| 1: Logistic regression adjusted for age, sex and smoking status (additive model) | | | | | | | |
| 2: Logistic regression adjusted for age and sex (additive model) | | | | | | | |
| 3: Logistic regression adjusted for age and sex (additive model) | | | | | | | |

# Rs4142441 is associated with the expression of OSER1-AS1 *in vitro*

To investigate whether rs4142441 was associated with the expression level of OSER1-AS1, we performed luciferase reporter assays in H1299 cells. We constructed a luciferase reporter vector containing the promoter region of OSER1-AS1 (1000bp on both sides of rs4142441). Two versions of the promoter sequences were constructed: rs4142441-WT (with allele A for rs4142441) or rs4142441-MUT (with allele G for rs4142441) (Fig. 1a). We observed that the expression of firefly luciferase fused to the promoter carrying rs4142441-MUT(G) was significantly lower than that of firefly luciferase fused to the promoter carrying rs4142441-WT(A) (Mann-Whitney U-test, $P = 0.0005$) (Fig. 1b**)**. To further validate the results, we constructed a pcDNA3.1 vector containing the WT and MUT rs4142441 alleles of OSER1-AS1 promoter sequence and the full-length cDNA sequence of OSER1-AS1 (Transcripts ID: ENST00000442383.1) (Fig. 1c). We transiently transfected the plasmids into H1299 cells and measured the OSER1-AS1 expression levels using qRT-PCR. OSER1-AS1 expression levels were significantly lower with vectors carrying rs4142441-MUT(G) allele (Mann-Whitney U-test, $P = 0.0041$) (Fig. 1d). Taken together, these pieces of evidence indicated that the allele G of rs4142441 was associated with down-regulation of OSER1-AS1.

# OSER1-AS1 down-regulation is associated with poor overall survival in TCGA LUAD patients

We measured the expression level of OSER1-AS1 in 129 paired NSCLC tumor and adjacent normal lung tissues using qRT-PCR. The clinical characteristic of the 129 NSCLC patients were summarized in **Supplementary Table S4**. We first examined the correlation between the expression level of OSER1-AS1 and clinical characteristics of the NSCLC patients. OSER1-AS1 was significantly lower among smokers ($P = 0.001$, **Supplementary Table S5).** Between the paired tumor and adjacent normal tissue, OSER1-AS1 expression levels were significantly down-regulated in NSCLC tumor tissues ($P = 0.0001$) (Fig. 2a, **left panel**). After stratifying samples by smoking status, the difference remained significant in the paired

tumor and adjacent normal lung tissues from the 90 smokers ($P$ = 0.0018) (Fig. 2a, **middle panel**) and 39 non-smokers ($P$ = 0.0052) (Fig. 2a, **right panel**).

We further assessed the clinical significance of OSER1-AS1 in NSCLC using the TCGA-LUAD RNA-seq dataset. Kaplan–Meier survival analysis was performed to investigate the association between OSER1-AS1 expression and patients' outcome. We observed that, in non-smokers, low expression of OSER1-AS1 was significantly associated with poor overall survival (n = 130, hazard ratio (HR) = 0.49 [95% CI 0.26–0.90]; $P$ = 0.022) (Fig. 2b, **right panel**). However, we found no significant association of OSER1-AS1 levels with overall survival in smokers or in the overall group. The association with overall survival in non-smoker patients remained marginally significant in multivariate Cox proportional-hazards regression after adjustment for age, sex, and tumor stage (n = 130, hazard ratio (HR) = 0.560 [95% CI 0.30–1.04]; $P$ = 0.066) (**Supplementary Table S6**). Collectively, these results revealed that the low expression levels of OSER1-AS1, which was associated with the allele G of rs4142441, were also associated with poor overall survival in TCGA-LUAD patients among non-smokers.

# Characterization of OSER1-AS1

OSER1-AS1 was located at chromosomal 20q13.12 and was coded on the positive strand. It consists of three exons with a full length of 1482 nt (**Supplementary Figures S2a**) (http://www.ncbi.nlm.nih.gov/RefSeq/).

We analyzed OSER1-AS1 expression levels in three NSCLC cell lines (H1299, A549 and SPCA1) by qRT-PCR, normalized to the expression level of β-actin. The H1299 cell line exhibited the highest OSER1-AS1 expression level, while A549 cell line exhibited the lowest OSER1-AS1 expression level (**Supplementary Figure S2b**). Therefore, we constructed a knocked down cell model of OSER1-AS1 expression in the H1299 and SPCA1 cell line in the following experiments, and constructed a gain-of-function cell model by transfecting an OSER1-AS1-overexpressing vector into the H1299, SPCA1 and A549 cell line.

ORFFinder predicted 4 short Open Reading Frames (ORFs) on the positive strand, which only codes short peptides of 29 to 66 amino acids (**Supplementary Figures S2c**) (https://www.ncbi.nlm.nih.gov/orffinder/). However, OSER1-AS1 lacks Kozak sequence, which is important for translation initiation. Moreover, OSER1-AS1 has no coding potential according to Coding Potential Calculator (CPC) (**Supplementary Figures S2d**) and Coding Potential Assessment Tool (CPAT) (Coding probability (CP) = 0.024) (CP > = 0.364 indicates coding sequence, CP < 0.364 indicates noncoding sequence) (**Supplementary Figure S2e**).

We further used an RNA fluorescence in situ hybridization (RNA-FISH) assay to investigate the subcellular localization of OSER1-AS1. OSER1-AS1 was predominantly observed in cell cytoplasm (**Supplementary Figure S3a**). The qRT-PCR qualification of nuclear and cytoplasmic RNA fractions further validated that OSER1-AS1 was mainly located in the cytoplasm (cytoplasm:nucleus ratio, 7:1) (**Supplementary Figure S3b**).

# OSER1-AS1 inhibits proliferation, migration, and invasion of NSCLC cells in vitro

To evaluate the potential role of OSER1-AS1 in NSCLC, we established gain-of-function cell models by transfecting pcDNA3.1-OSER1-AS1 expressing vectors into the H1299 and SPCA1 cells (**Supplementary Figure S4a**). In addition, we transfected H1299 and SPCA1 cells with two siRNAs targeting independent regions of OSER1-AS1 to investigate the effect of down-regulation of OSER1-AS1 on cell proliferation, migration and invasion (**Supplementary Figure S4b**). We examined the effects of OSER1-AS1 overexpression on cell proliferation, migration and invasion. CCK-8 assays showed that overexpression of OSER1-AS1 significantly decreased the proliferation of H1299 and SPCA1 cells (**Supplementary Figure S5a**). Moreover, the *in vitro* transwell assays showed that overexpression of OSER1-AS1 significantly decreased the migration and invasion of H1299 and SPCA1 cells compared with vector control (**Supplementary Figure S5c, d**). The down-regulation of OSER1-AS1 significantly increased the proliferation, migration and invasion of H1299 and SPCA1 cells compared with vector control (**Supplementary Figure S5b, e, f**).

# OSER1-AS1 represses tumor growth and metastasis *in vivo*

To investigate whether OSER1-AS1 suppresses tumorigenesis *in vivo*, we implanted A549 cells stably transfected with OSER1-AS1 or control vector subcutaneously in immunodeficiency mice. The tumor mass and volume in OSER1-AS1 overexpression group were significantly smaller and lighter than those in control group (Fig. 3a, **b and c**). To validate the anti-metastatic effects of OSER1-AS1 in vivo, A549 cells stably transfected with OSER1-AS1 or control vector were injected into the tail veins of nude mice. The number of metastatic nodules on the surface of the lung was significantly decreased in mice receiving OSER1-AS1 stable overexpressing A549 cells compared with the control group (Fig. 3d). Hematoxylin and eosin (H&E) staining of the mice lung tissue slice confirmed that less metastatic nodules were present in the OSER1-AS1 overexpression group than the control group. Furthermore, proliferation marker Ki-67 was evaluated through immunohistochemistry in tumor tissues. Ki-67 expression levels were also significantly lower in OSER1-AS1 overexpression group than those in control vector group (Fig. 3e).

# OSER1-AS1 promoter is suppressed by MYC

To explore the potential transcription factor that regulates the expression of OSER1-AS1, we searched the Transcription Factor ChIP-seq from ENCODE (Txn Factor ChIP) track in the UCSC genome browser. We found a binding site for MYC within the OSER1-AS1 promoter region (-333 bp ~ + 116 bp TSS of OSER1-AS1), covering rs4142441 (Fig. 4a). Thus, we then examined the regulation effect of MYC on OSER1-AS1 expression. By using ChIP experiments, we confirmed the direct interaction of MYC to OSER1-AS1 promoter using two pairs of primers binding to different positions of the potential binding region of MYC (Fig. 4b **& c**). We next performed luciferase reporter assays to further investigate the effect of the WT and MUT alleles of rs4142441 on the regulatory efficiency of MYC. The sequences of OSER1-AS1 promoter region (-1000 bp ~ + 1000 bp) were inserted into the reporter plasmid. Co-transfection of the MYC-overexpression vectors with OSER1-AS1 promoter luciferase construct significantly repressed the luciferase activity. Moreover, the luciferase activity from the promoter carrying rs4142441-MUT(G) was significantly lower than that of firefly luciferase fused to the promoter carrying rs4142441-MUT(A), both

with or without MYC co-transfection ($P < 0.0001$) (Fig. 4d**)**. In addition, we transiently transfected the MYC overexpression plasmids into H1299 cells and measured the OSER1-AS1 expression levels using qRT-PCR. The results from qRT-PCR showed that MYC-overexpression vectors significantly decreased the expression of OSER1-AS1 in comparison to the control vector ($P < 0.05$) (Fig. 4e**)**. These lines of evidence demonstrated that MYC suppressed the transcription of OSER1-AS1, and the allele G of rs4142441 was associated with down-regulation of OSER1-AS1 regardless of the binding status of MYC.

# OSER1-AS1 3’-end is bound by microRNA hsa-miR-17-5p and RNA-binding protein ELAVL1

Previous studies have reported that MYC could up-regulate hsa-miR-17-5p, which in turn mediated MEK inhibitor resistance in AZD6244 treatment in lung cancer cell lines [19–21]. Therefore, we searched public database (http://starbase.sysu.edu.cn/) to look for the potential binding site of hsa-miR-17-5p in the 3’-end of OSER1-AS1. One binding site to hsa-miR-17-5p in the 3’-end of OSER1-AS1 was supported by high-throughput sequencing of RNA isolated by crosslinking immunoprecipitation (HITS-CLIP) experiment (GEO accession: GSM2065794. Target site (hg19): chr20:42854367–42854385[+] (**Supplementary Figure S6a**).

In addition, up- and down-stream in close proximity of this hsa-miR-17-5p target site, 4 binding sites of RNA-binding protein ELAVL1 (ELAV-like protein 1 or ELAVL1) were reported by independent CLIP-seq experiments (**Supplementary Figure S6b**). ELAVL1 was an widely studied RNA-binding protein that played a role in promoting cell proliferation by stabilizing mRNAs of oncogenes involved in cell cycle regulation [22]. Therefore, we next explored the impacts of hsa-miR-17-5p and ELAVL1 binding on the expression levels of OSER1-AS1. We first investigated the differential luciferase activity of Pischeck-2 vector containing the OSER1-AS1 3’-end region co-transfected with hsa-miR-17-5p mimic, NC mimic, inhibitor and NC-inhibitor. We found out that hsa-miR-17-5p mimics significantly reduced the luciferase activities of the Pischeck-2 reporter containing the OSER1-AS1 3’-end region, whereas inhibitors of hsa-miR-17-5p caused the opposite effect **(Supplementary Figure S6c)**. Subsequently, we investigated the expression levels of OSER1-AS1 after transfection with hsa-miR-17-5p mimic, NC mimic, inhibitor and NC-inhibitor. The miR-17-5p inhibitors significantly increased OSER1-AS1 expression levels, whereas the miR-17-5p mimics significantly decreased OSER1-AS1 in H1299 cells compared with control (**Supplementary Figure S6d**). In contrast, after overexpression or knockdown of OSER1-AS1 in H1299 cells, miR-17-5p were down-regulated or up-regulated, respectively (**Supplementary Figure S6e**). Then we co-transfected ELAVL1 plasmids with hsa-miR-17-p mimics in luciferase assays. ELAVL1 alone significantly increased the luciferase activities of the OSER1-AS1 3’-end reporter vector, but when co-transfecting ELAVL1 plasmids with hsa-miR-17-5p mimics, the luciferase activities were down-regulated in comparison to transfecting with ELAVL1 plasmids alone **(Supplementary Figure S6f).**

# OSER1-AS1 sequesters ELAVL1 by direct lncRNA-protein interaction

We next investigated the biological mechanism by which OSER1-AS1 suppressing tumorigenesis. The activity of ELAVL1 has been known to be dependent on its subcellular distribution: it predominantly localizes within the nucleus of resting cells. Under certain biological circumstances, it transports to the cytoplasm and binds to its target mRNA's 3'UTR [23]. The ELAVL1-mRNA complex would prevent the mRNA from degradation and thereby increase its translational level [24]. Since OSER1-AS1 were distributed predominantly in cell cytoplasm (**Supplementary Figure S3**), we hypothesized that it might function as natural sponges to prevent ELAVL1 from binding its target mRNAs in the cytoplasm.

We performed RNA immunoprecipitation (RIP) experiment to pull down the endogenous OSER1-AS1-protein complex in H1299 cell line. We used both ELAVL1 and AGO2 antibodies to pull down OSER1-AS1, because OSER1-AS1 was not only bound by ELAVL1 but also by hsa-miR-17-5p, and AGO2 was the catalytic center of the RNA-induced silencing complex (RISC)[25]. To determine the relative binding abundances of OSER1-AS1-ELALV1 complex and OSER1-AS1-AGO2 complex in subcellular compartment, we separated the nuclear and cytoplasmic fractions from RIP lysates. The results showed that OSER1-AS1-ELAVL1 complex was approximately 4 folds more enriched than the OSER1-AS1-AGO2 complex in the whole cell. While in the nucleus, OSER1-AS1 was also preferentially bound to ELAVL1 (OSER1-AS1-ELAVL1 complex to OSER1-AS1-AGO2 complex ratio 5:1). However, the cytoplasmic OSER1-AS1 was predominantly bound by AGO2 (OSER1-AS1-ELAVL1 complex to OSER1-AS1-AGO2 complex ratio 1:70) (Fig. 5a).

To further investigate the potential influence of OSER1-AS1 on the subcellular localization of ELAVL1, we performed western blot in whole cell, nuclear and cytoplasmic cell lysate prepared from H1299 cells transfected with scramble siRNA (NC), two separate siRNAs targeting OSER1-AS1 (siRNA-323 and siRNA-373), stable empty vector and OSER1-AS1 overexpression vector. Consistent with the previous studies, our results showed that ELAVL1 was predominantly distributed in the nucleus, and AGO2 was in both nucleus and cytoplasm [23]. Although we found no significant alteration of ELAVL1 and AGO2 expressions in the whole cell, OSER1-AS1 changed the subcellular localization of ELAVL1. Knockdown of OSER1-AS1 attenuated the translocation of ELAVL1 from nucleus to cytoplasm in H1299 cells, whereas OSER1-AS1 overexpression increased the amount of cytoplasmic ELAVL1 proteins (Fig. 5b).

Our findings in RIP and western blot experiments together suggested that OSER1-AS1 directly bound with ELAVL1 and the up-regulation of OSER1-AS1 caused the accumulation of ELAVL1 proteins in the cytoplasm.

# OSER1-AS1 regulates the target genes of ELAVL1 and miR-17-5p

MYC has been reported to stimulate the expression of microRNAs in the miR-17–92 cluster, including miR-17-5p [26–28], which in turn suppressed the expression of the pro-apoptotic protein BCL2L11 in lymphoma [29] and in NSCLC [30]. On the other hand, the RBP ELAVL1 was known to up-regulate the translational level of MYC [31–33]. Considering that the 3'-end of OSER1-AS1 was bound by both miR-17-5p and ELAVL1, we hypothesized that OSER1-AS1 could act as a miR-17-5p sponge to change the

expression of its target gene BCL2L11. By the same theory, OSER1-AS1 may also sponge ELAVL1 away from its target MYC mRNAs, leading to decreased translational efficiency and decreased MYC protein levels. Hence, we performed western blot to assess MYC and BCL2L11 protein level after knockdown and overexpression of OSER1-AS1. The result of western blotting indicated that knockdown of OSER1-AS1 increased the MYC expression, whereas the overexpression of OSER1-AS1 decreased the MYC expression. The change of MYC expression was more profound in the nucleus, consistent with the knowledge that MYC was a transcription factor that mainly executed its functions in the nucleus [28]. The influence of OSER1-AS1 on the BCL2L11 expression was in the opposite direction: knockdown of OSER1-AS1 decreased the BCL2L11 expression, whereas the overexpression of OSER1-AS1 increased the BCL2L11 expression. The pattern of BCL2L11 expression change was similar in the nuclear and cytoplasmic fraction, consistent with the knowledge that BCL2L11 was distributed both in the cytoplasm and in the nucleus **(Fig. 6)**.

# Discussion

In this study, we tested a list of SNPs located near lncRNAs to detect their associations with lung cancer risks. From one significantly associated SNP rs4142441, we narrowed down our focus to lncRNA OSER1-AS1. We demonstrated that the mutant allele (G) of rs4142441 was associated with higher lung cancer risk and lower expression level of OSER1-AS1. Rs4142441 was previously reported in a large-scale GWAS study as associated with monocyte count in whole blood. The allele G was associated with increased monocyte count (Beta coefficient = 0.033; [95% CI 0.023–0.043]; $P = 4 \times 10^{-11}$) [34]. An elevated peripheral monocyte count has been reported to have a poor prognosis impact on lung adenocarcinoma [35].

The qRT-PCR analysis confirmed OSER1-AS1 was significantly down-regulated in lung adenocarcinoma tissues in comparison to adjacent normal tissues. Moreover, the differential expression was more profound among non-smokers. Therefore, we hypothesized that OSER1-AS1 played a tumor suppressive role in NSCLC. We then investigated the prognostic value of OSER1-AS1 using clinical data from TCGA public database by Kaplan-Meier survival analysis. We found that high expression of OSER1-AS1 was associated with better overall survival in TCGA-LUAD non-smoker patients. In addition, OSER1-AS1 suppressed lung cancer cells proliferation, migration, and invasion *in vitro* and promoted tumorigenesis *in vivo*.

Furthermore, our results showed that transcription factor MYC suppressed OSER1-AS1 expression. Transcription factor MYC was a commonly known regulator which activated growth-related genes and suppressed genes involved in cell cycle arrest, cell adhesion, and cell–cell communication [36]. In addition, MYC was up-regulated in human NSCLC cells [37, 38] and MYC depletion has been reported to be able to reverses immune evasion and enables effective treatment of lung cancer [39]. MYC was known to bind to the core promoter of the genes it repressed directly [40], and itself has been known to be regulated by a number of lncRNAs [41]. The results from our ChIP experiment confirmed the directing binding of MYC at the promoter region of OSER1-AS1. The binding site of MYC covered the SNP rs4142441, but its allelic status did not interfere with MYC binding capacity. One possible explanation was that rs4142441 influenced the expression level of OSER1-AS1 via other transcription factors such as

RNA polymerase II. The exact biological mechanism that may cause the association between allele G of rs4142441 and the lower expression level of OSER1-AS1 remains to be explored.

One the other hand, the 3’-end of OSER1-AS1 was bound competitively by hsa-miR-17-5p and RNA-binding protein ELAVL1. The RNA sequence of OSER1-AS1 contained more than 9 ARE motifs required for ELAVL1 binding, and the nearest ARE motif was only 51 bp 5' upstream of the miR-17-5p binding site.

Some studies have implicated the roles of ELAVL1 in affecting the binding capacity of AGO2 and miRNAs [23], and the effects could be either a competition[42] or cooperation[43, 44], probably depending on the conformational changes of the 3’UTR caused by the initial binding. In the study of Chang et al. (2013), ELAVL1 has been reported to antagonize the suppressive effect of miR-200b on VEGF-A expression by competitive binding [45]. However, unlike VEGF-A, OSER1-AS1 as a lncRNA cannot be stabilized by ELAVL1 and translated into proteins. Therefore, we hypothesized that OSER1-AS1 may execute its biological function as a decoy by forming a stable RNA-protein complex with ELAVL1 and sequestering it from its target mRNAs.

Several studies had shown that some lncRNAs could serve as a sponge to restrict RBPs’ availability to its target mRNAs [46–48]. The post-transcriptional regulations by ELAVL1 mainly took place in the cytoplasm [49]. Our RNA FISH assays demonstrated that OSER1-AS1 located mainly in the cytoplasm (cytoplasm:nucleus ratio 7:1), so the subcellular localization of OSER1-AS1 was consistent with our “ELAVL1 sponge” hypothesis.

To test this hypothesis, we performed RIP assays in the whole cell lysate, nuclear lysate, and cytoplasmic lysate separately. The results from RIP experiments confirmed that physical interaction happened between OSER1-AS1 and ELAVL1. In the whole cell, OSER1-AS1 preferentially formed RBP-RNA complex with ELAVL1. Moreover, OSER1-AS1 was also bound by AGO2, which is consistent with our finding that OSER1-AS1 was targeted by hsa-miR-17-5p. In the nucleus, OSER1-AS1 was predominantly bound by ELAVL1. However, in the cytoplasm, OSER1-AS1 was mainly bound by AGO2, suggesting it was under the suppressive status in RISC complexes in the cytoplasm. This seems to be counter-intuitive to our “ELAVL1 sponge” hypothesis, because ELAVL1 was known to carry out its mRNA stabilizer function in the cytoplasm. One possible explanation could be that ELAVL1 mainly localized in the nucleus, the cytoplasmic level of ELAVL1 was extremely low so the presence ELAVL1-OSER1-AS1 complex would be difficult to be accurately quantified in RIP assays.

Then we interfered the expression level of OSER1-AS1 to explore further on whether OSER1-AS1 had any impact on the ELAVL1 protein level. Our results indicated that, although OSER1-AS1 had no significant influence on the overall protein level of ELAVL1, it changed its subcellular localization. Overexpression of OSER1-AS1 resulted in the accumulation of ELAVL1 proteins in the cytoplasm, whereas the knockdown of OSER1-AS1 caused the opposite effect. However, this was in conflict with the findings from previous studies which showed higher cytoplasmic level of ELAVL1 associated with increased tumorigenic activity and poor prognostic outcome in NSCLC [50, 51]. One possible explanation might be that, even though

OSER1-AS1 increased the cytoplasmic level of ELAVL1, these ELAVL1 were not functional because they were not be able to bind their target mRNAs, and they could not be transported back to the nucleus.

Subsequently, we investigated whether OSER1-AS1 changed the level of MYC, which was both a regulator of OSER1-AS1 and a target gene of ELAVL1. We found that the knockdown of OSER1-AS1 increased the MYC expression, whereas the overexpression of OSER1-AS1 decreased the MYC expression. Taking together with the finding that MYC suppressed the transcriptional level of OSER1-AS1, we concluded that MYC and OSER1-AS1 controlled each other in a negative feedback loop (Fig. 7). In addition, we found that OSER1-AS1 positively regulate the expression level of BCL2L11, which was targeted by miR-17-5p, further validating the hypothesis that OSER1-AS1 functioned as a miRNA sponge of miR-17-5p.

Taking together, we demonstrated that OSER1-AS1 exercised tumor suppressive functions in NSCLC by acting as an ELAVL1 decoy and sequestered ELAVL1 from its target mRNAs involved in cell proliferation, migration and tumorigenicity. In company with previous studies [22, 23, 52, 53], we showed that ELAVL1 can bind to the 3'-end of lncRNA OSER1-AS1 in competition with a microRNA hsa-miR-17-5p. These findings highlighted that, other than sponging microRNAs, another possible mechanism of lncRNAs to exercise its tumor-suppressing function might be sponging oncogenic RBPs away from its target mRNAs.

# Conclusion

Our study demonstrates that OSER1-AS1 is down-regulated in tumor and acts as a tumor suppressor in NSCLC. OSER1-AS1 is co-regulated by SNP rs4142441 and MYC at the promoter, and competitively targeted by both microRNA hsa-miR-17-5p and RBP ELAVL1 at the 3'-end. It performs tumor suppressive function by forming an RNA-protein complex with ELAVL1 and sequester it from binding and stabilizing its target mRNAs, numerous of which are implicated in carcinogenesis. Our results suggest that OSER1-AS1 could play important roles in ELAVL1-regulated mRNA stability. These findings could provide biological insight into the regulation of the ceRNA network in NSCLC, and give new clues for future development of new therapeutic targets and biomarkers.

# Abbreviations

ACTB, Beta-actin; CCK-8, Cell Counting Kit-8; ceRNA, competitive endogenous RNA; CHIP, chromatin immunoprecipitation; CI, confidence interval; CPAT, coding potential assessment tool; CPC, coding potential calculator; ELAVL1, ELAV Like RNA Binding Protein 1; EMT, Epithelial-mesenchymal transition; FISH, fluorescence in situ hybridization; NC, Negative control; HR, hazard ratio; H&E, hematoxylin and eosin; lncRNA, long noncoding RNA; HuR, Human antigen R; miRNA, microRNA; MUT, mutant type; NSCLC, non-small cell lung cancer; ORF, open reading frame; OS, Overall survival; qRT-PCR, quantitative real-time PCR; siRNA, small interfering RNA; RBP, RNA Binding Protein; RISC,RNA-induced silencing complex; RIP,RNA Immunoprecipitation; TSS, transcription start site; UTR, untranslated region; WB, western blot; WT, wild type.

# Declarations


## Acknowledgements

Not applicable.


## Authors' contributions

Y.L. led the study by designing, conducting, interpreting results, writing the manuscript, and obtaining the funding. W.X. performed the majority of the experiments and participated in study design, result interpretation, manuscript writing, and obtaining the funding. Y. W. performed the experiments and coordinated result interpretation and manuscript writing. Y.Z. participated in study design, performed the experiments, participated in result interpretation, and manuscript writing. L.B. and Z.Y. participated in study design, participant recruitment, result interpretation, and funding support. Y.X. performed plasmid construction and cell transfection. C.L. collected human tissue samples and clinical data and performed animal experiments. W.N. performed the bioinformatics analysis. N.W. and L.W. participated in data collection and laboratory work. T.C. and X.M. contributed to results interpretation and discussions. All authors contributed to the final paper.


## Funding

This work was supported by the National Natural Science Foundation of China (No. 81602933 to W. X.; No. 81672316, 81472190 and 81171903 to Y. L.; No. 81370139 to L. B.) and foundation for Clinical Research from Xinqiao Hospital, Third Military Medical University (No. 2014YLC13 to L. B., No. 2015YLC21 to Z. Y.)


## Availability of data and materials

The case control datasets generated and/or analysed during the current study are not publicly available due to individual privacy but are available from the corresponding author on reasonable request and with permission of the Department of Respiratory Disease of Xinqiao Hospital. The TCGA-LUAD datasets analysed in the study are openly available in the GDC data portal (https://portal.gdc.cancer.gov/repository).

## Ethics approval and consent to participate

All experimental animal procedures were approved by the Institutional Animal Care and Use Committee of Third Military Medical University. All subjects provided informed written consent. Research protocol was approved by the ethics committee of the Army Medical University.

## Consent for publication

Not applicable.

### Competing interests

The authors declare that they have no competing interests.

# References


1. Torre LA, Bray F, Siegel RL, Ferlay J, Lortet-Tieulent J, Jemal A. Global cancer statistics, 2012. CA Cancer J Clin. 2015;65(2):87-108.
2. Ettinger DS, et al. Non-small cell lung cancer, version 2.2013. J Natl Compr Canc Netw. 2013;11(6):645-53; quiz 53.
3. Borczuk AC, Toonkel RL, Powell CA. Genomics of lung cancer. Proc Am Thorac Soc. 2009;6(2):152-8.
4. Davidson MR, Gazdar AF, Clarke BE. The pivotal role of pathology in the management of lung cancer. J Thorac Dis. 2013;5 Suppl 5:S463-78.
5. Xie W, Yuan S, Sun Z, Li Y. Long noncoding and circular RNAs in lung cancer: advances and perspectives. Epigenomics. 2016;8(9):1275-87.
6. Mascaux C, Tsao MS, Hirsch FR. Genomic Testing in Lung Cancer: Past, Present, and Future. J Natl Compr Canc Netw. 2018;16(3):323-34.
7. Yuan S, et al. Long non-coding RNA MUC5B-AS1 promotes metastasis through mutually regulating MUC5B expression in lung adenocarcinoma. Cell Death Dis. 2018;9(5):450.
8. Yuan S, et al. Hypoxia-sensitive LINC01436 is regulated by E2F6 and acts as an oncogene by targeting miR-30a-3p in non-small cell lung cancer. Mol Oncol. 2019;13(4):840-56.
9. Chen S, et al. Roles of MYC-targeting long non-coding RNA MINCR in cell cycle regulation and apoptosis in non-small cell lung Cancer. Respir Res. 2019;20(1):202.
10. Hua Q, et al. LINC01123, a c-Myc-activated long non-coding RNA, promotes proliferation and aerobic glycolysis of non-small cell lung cancer through miR-199a-5p/c-Myc axis. J Hematol Oncol. 2019;12(1):91.
11. Bosse Y, Amos CI. A Decade of GWAS Results in Lung Cancer. Cancer Epidemiol Biomarkers Prev. 2018;27(4):363-79.
12. Sun C, et al. Long non-coding RNA NEAT1 promotes non-small cell lung cancer progression through regulation of miR-377-3p-E2F3 pathway. Oncotarget. 2016;7(32):51784-814.
13. Schmitt AM, Chang HY. Long Noncoding RNAs in Cancer Pathways. Cancer Cell. 2016;29(4):452-63.
14. Fang J, Sun CC, Gong C. Long noncoding RNA XIST acts as an oncogene in non-small cell lung cancer by epigenetically repressing KLF2 expression. Biochem Biophys Res Commun. 2016;478(2):811-7.
15. Zhou X, et al. Diagnostic value of a plasma microRNA signature in gastric cancer: a microRNA expression analysis. Sci Rep. 2015;5:11251.
16. Liu X, et al. miR-30a acts as a tumor suppressor by double-targeting COX-2 and BCL9 in H. pylori gastric cancer models. Sci Rep. 2017;7(1):7113.

17. Yuan S, et al. GPC5, a novel epigenetically silenced tumor suppressor, inhibits tumor growth by suppressing Wnt/beta-catenin signaling in lung adenocarcinoma. Oncogene. 2016;35(47):6120-31.
18. Liu WB, et al. Epigenetic silencing of cell cycle regulatory genes during 3-methylcholanthrene and diethylnitrosamine-induced multistep rat lung cancer. Mol Carcinog. 2010;49(6):556-65.
19. Li Y, Choi PS, Casey SC, Dill DL, Felsher DW. MYC through miR-17-92 suppresses specific target genes to maintain survival, autonomous proliferation, and a neoplastic state. Cancer Cell. 2014;26(2):262-72.
20. Aguda BD, Kim Y, Piper-Hunter MG, Friedman A, Marsh CB. MicroRNA regulation of a cancer network: consequences of the feedback loops involving miR-17-92, E2F, and Myc. Proc Natl Acad Sci U S A. 2008;105(50):19678-83.
21. Chen L, et al. miR-17-92 cluster microRNAs confers tumorigenicity in multiple myeloma. Cancer Lett. 2011;309(1):62-70.
22. Wang W, Caldwell MC, Lin S, Furneaux H, Gorospe M. HuR regulates cyclin A and cyclin B1 mRNA stability during cell proliferation. EMBO J. 2000;19(10):2340-50.
23. Srikantan S, Tominaga K, Gorospe M. Functional interplay between RNA-binding protein HuR and microRNAs. Curr Protein Pept Sci. 2012;13(4):372-9.
24. Wang J, Guo Y, Chu H, Guan Y, Bi J, Wang B. Multiple functions of the RNA-binding protein HuR in cancer progression, treatment responses and prognosis. Int J Mol Sci. 2013;14(5):10015-41.
25. Martinez NJ, Gregory RI. Argonaute2 expression is post-transcriptionally coupled to microRNA abundance. Rna. 2013;19(5):605-12.
26. Kumar P, Luo Y, Tudela C, Alexander JM, Mendelson CR. The c-Myc-regulated microRNA-17~92 (miR-17~92) and miR-106a~363 clusters target hCYP19A1 and hGCM1 to inhibit human trophoblast differentiation. Mol Cell Biol. 2013;33(9):1782-96.
27. Ventura A, et al. Targeted deletion reveals essential and overlapping functions of the miR-17 through 92 family of miRNA clusters. Cell. 2008;132(5):875-86.
28. Psathas JN, Thomas-Tikhonenko A. MYC and the art of microRNA maintenance. Cold Spring Harb Perspect Med. 2014;4(8).
29. Xiao C, et al. Lymphoproliferative disease and autoimmunity in mice with increased miR-17-92 expression in lymphocytes. Nat Immunol. 2008;9(4):405-14.
30. Dai B, et al. STAT3 mediates resistance to MEK inhibitor through microRNA miR-17. Cancer Res. 2011;71(10):3658-68.
31. Hatanaka T, Higashino F, Tei K, Yasuda M. The neural ELAVL protein HuB enhances endogenous proto-oncogene activation. Biochem Biophys Res Commun. 2019;517(2):330-7.
32. Perrone EE, Liu L, Turner DJ, Strauch ED. Bile salts increase epithelial cell proliferation through HuR-induced c-Myc expression. J Surg Res. 2012;178(1):155-64.
33. Kakuguchi W, et al. HuR knockdown changes the oncogenic potential of oral cancer cells. Mol Cancer Res. 2010;8(4):520-8.

34. Astle WJ, et al. The Allelic Landscape of Human Blood Cell Trait Variation and Links to Common Complex Disease. Cell. 2016;167(5):1415-29 e19.
35. Kumagai S, et al. Prognostic impact of preoperative monocyte counts in patients with resected lung adenocarcinoma. Lung Cancer. 2014;85(3):457-64.
36. Eilers M, Eisenman RN. Myc's broad reach. Genes Dev. 2008;22(20):2755-66.
37. Li H, et al. C-myc/miR-150/EPG5 axis mediated dysfunction of autophagy promotes development of non-small cell lung cancer. Theranostics. 2019;9(18):5134-48.
38. Mustachio LM, Roszik J, Farria AT, Guerra K, Dent SY. Repression of GCN5 expression or activity attenuates c-MYC expression in non-small cell lung cancer. Am J Cancer Res. 2019;9(8):1830-45.
39. Topper MJ, et al. Epigenetic Therapy Ties MYC Depletion to Reversing Immune Evasion and Treating Lung Cancer. Cell. 2017;171(6):1284-300 e21.
40. Herkert B, Eilers M. Transcriptional repression: the dark side of myc. Genes Cancer. 2010;1(6):580-6.
41. Swier L, Dzikiewicz-Krawczyk A, Winkle M, van den Berg A, Kluiver J. Intricate crosstalk between MYC and non-coding RNAs regulates hallmarks of cancer. Mol Oncol. 2019;13(1):26-45.
42. Chen Y, et al. Circular RNA circAGO2 drives cancer progression through facilitating HuR-repressed functions of AGO2-miRNA complexes. Cell Death Differ. 2019;26(7):1346-64.
43. Balkhi MY, et al. miR-29 acts as a decoy in sarcomas to protect the tumor suppressor A20 mRNA from degradation by HuR. Sci Signal. 2013;6(286):ra63.
44. Sun Q, et al. MIR100 host gene-encoded lncRNAs regulate cell cycle by modulating the interaction between HuR and its target mRNAs. Nucleic Acids Res. 2018;46(19):10405-16.
45. Chang SH, et al. Antagonistic function of the RNA-binding protein HuR and miR-200b in post-transcriptional regulation of vascular endothelial growth factor-A expression and angiogenesis. J Biol Chem. 2013;288(7):4908-21.
46. Kim J, et al. LncRNA OIP5-AS1/cyrano sponges RNA-binding protein HuR. Nucleic Acids Res. 2016;44(5):2378-92.
47. Zhang F, Ni H, Li X, Liu H, Xi T, Zheng L. LncRNA FENDRR attenuates adriamycin resistance via suppressing MDR1 expression through sponging HuR and miR-184 in chronic myelogenous leukaemia cells. FEBS Lett. 2019;593(15):1993-2007.
48. Shen L, et al. Cachexia-related long noncoding RNA, CAAlnc1, suppresses adipogenesis by blocking the binding of HuR to adipogenic transcription factor mRNAs. Int J Cancer. 2019;145(7):1809-21.
49. Tirosh I. Transcriptional priming of cytoplasmic post-transcriptional regulation. Transcription. 2011;2(6):258-62.
50. Wang J, Wang B, Bi J, Zhang C. Cytoplasmic HuR expression correlates with angiogenesis, lymphangiogenesis, and poor outcome in lung cancer. Med Oncol. 2011;28 Suppl 1:S577-85.
51. Wang J, et al. The expression of RNA-binding protein HuR in non-small cell lung cancer correlates with vascular endothelial growth factor-C expression and lymph node metastasis. Oncology. 2009;76(6):420-9.

52. Tominaga K, et al. Competitive regulation of nucleolin expression by HuR and miR-494. Mol Cell Biol. 2011;31(20):4219-31.
53. Epis MR, Barker A, Giles KM, Beveridge DJ, Leedman PJ. The RNA-binding protein HuR opposes the repression of ERBB-2 gene expression by microRNA miR-331-3p in prostate cancer cells. J Biol Chem. 2011;286(48):41442-54.

# Figures

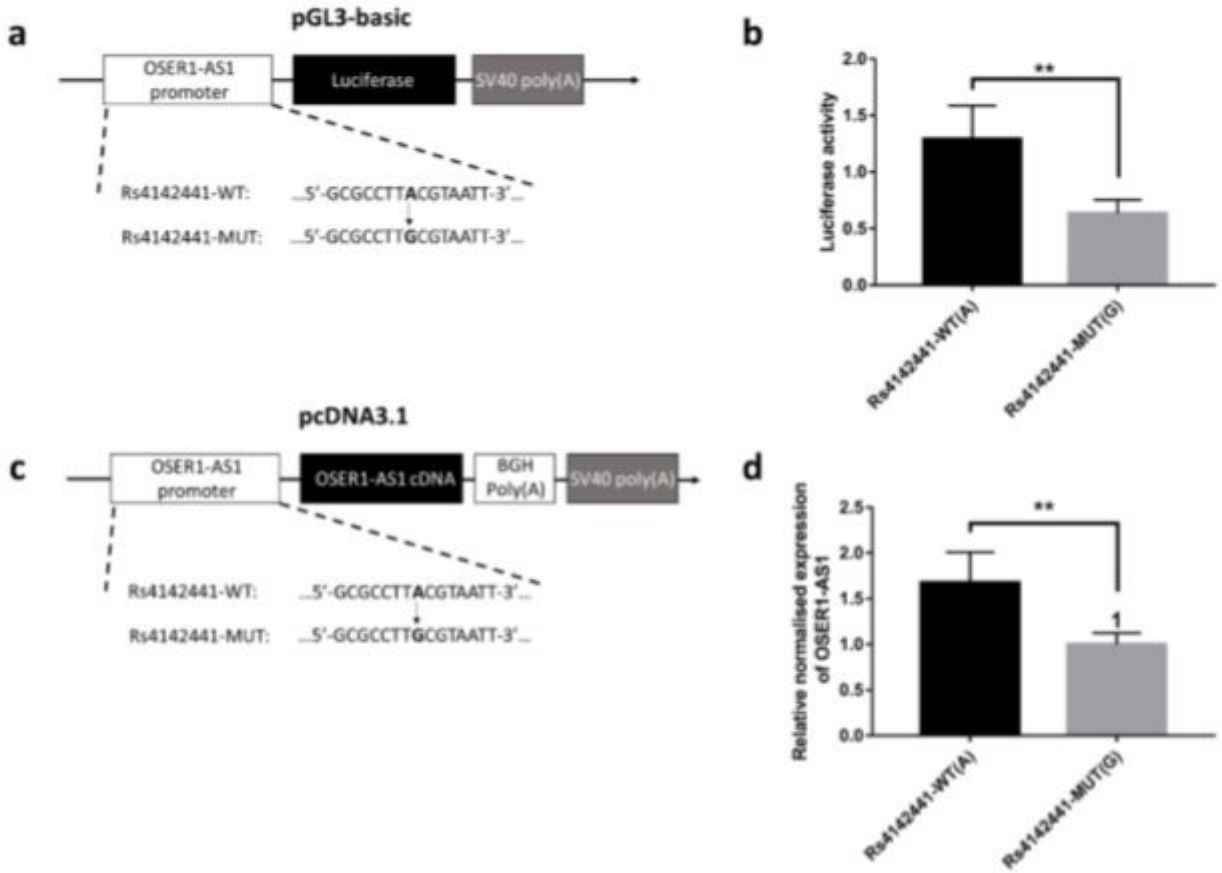


**Figure 1**

Rs4142441-MUT is associated with decreased expression of lncRNA OSER1-AS1. (a) The pGL3 firefly luciferase reporter plasmids with wild-type or mutant allele for rs4142441. Rs4142441-WT represents the sequence with the wild type allele (A) of rs4142441. Rs4142441-MUT represents the sequence with the mutant allele (G) of rs4142441. (b) The pGL3 firefly luciferase reporter plasmids with wild-type or mutant allele for rs4142441 were transiently transfected into H1299 cells with a Renilla luciferase reporter for normalization. Luciferase activities were measured after 48 hr. The data were presented as the means and the standard deviations (SDs) of separate transfections (n = 3). Error bars represent the SD. ** Mann-Whitney U-test, $P < 0.01$. (c) The pcDNA3.1 plasmid with its CMV promoter replaced by the promoter region of OSER1-AS1 (±1000bp on both sides of rs4142441). Rs4142441-WT represents the sequence

with the wild type allele (A) of rs4142441. Rs4142441-MUT represents the sequence with the mutant allele (G) of rs4142441. The cDNA sequence of OSER1-AS1 (Transcripts ID: ENST00000442383.1) was inserted into the multiple cloning site. (d) OSER1-AS1 expression levels were measured after 48 hr of transfection. The relative normalized expression level was calculated as the fold change of the expression level of rs4142441-WT(A) vector relative to rs4142441-MUT(G), normalized to the expression level of β-actin. The data were presented as the means and the standard deviations (SDs) of separate transfections (n = 3). Error bars represent the SD. ** Mann-Whitney U-test, P < 0.01.

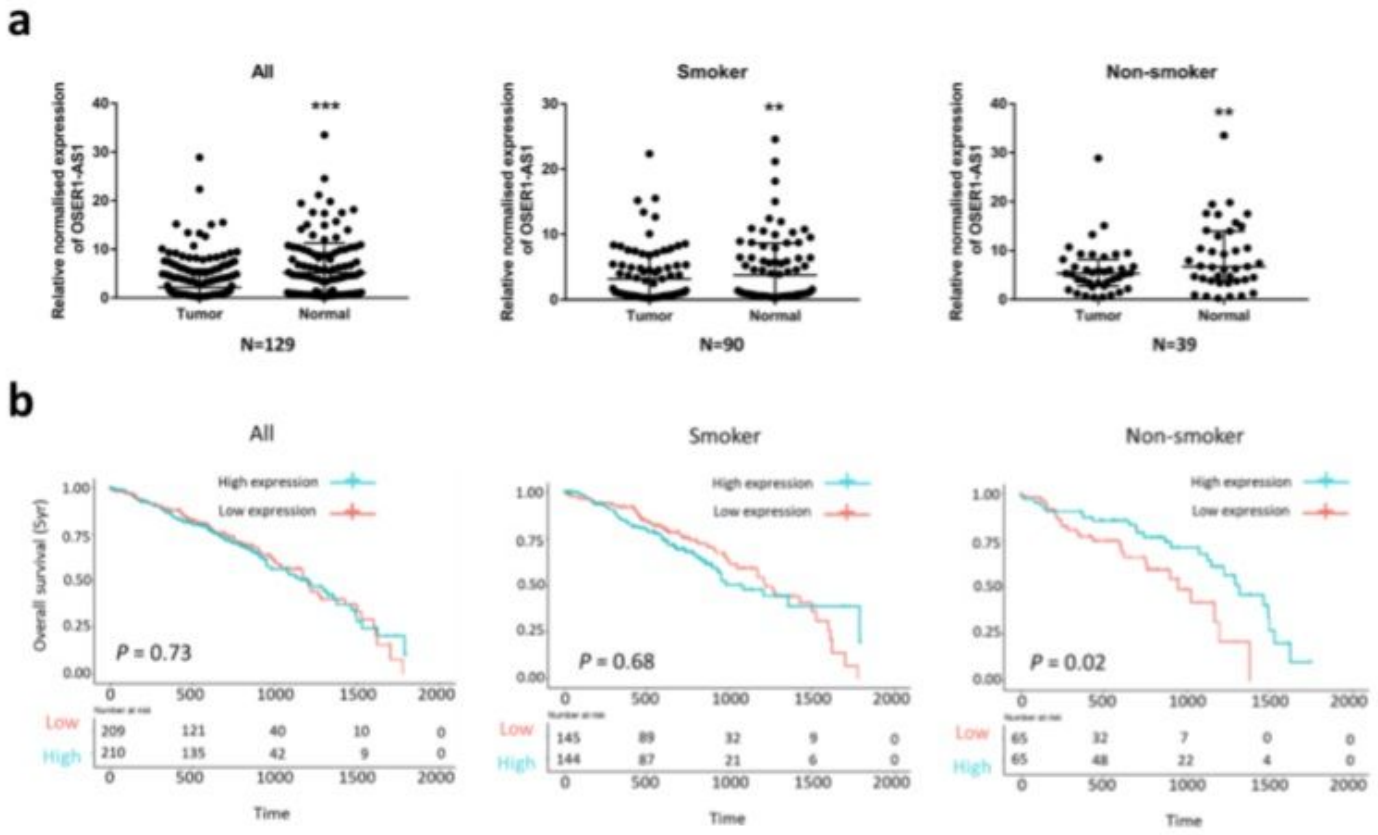


## Figure 2

OSER1-AS1 expression is down-regulated in NSCLC tissues and associated with poor overall survival in TCGA LUAD patients. (a) The qRT-PCR analysis of relative OSER1-AS1 expression in NSCLC tissues compared with paired adjacent normal lung tissues. Left panel: all group. Middle panel: smoker group. Right panel: non-smoker group. The differential expression between tumor and adjacent normal lung tissue was compared using Wilcoxon matched pairs signed rank test: **, P < 0.01; ***, P < 0.001. (b) Kaplan-Meier curves for overall survival (OS) of TCGA-LUAD patients expressing high and low expression levels of OSER1-AS1. Left panel: overall group. Middle panel: smoker group. Right panel: non-smoker group. The difference in survival between high and low expression groups (divided by median OSER1-AS1 expression value) were compared using the log-rank test.

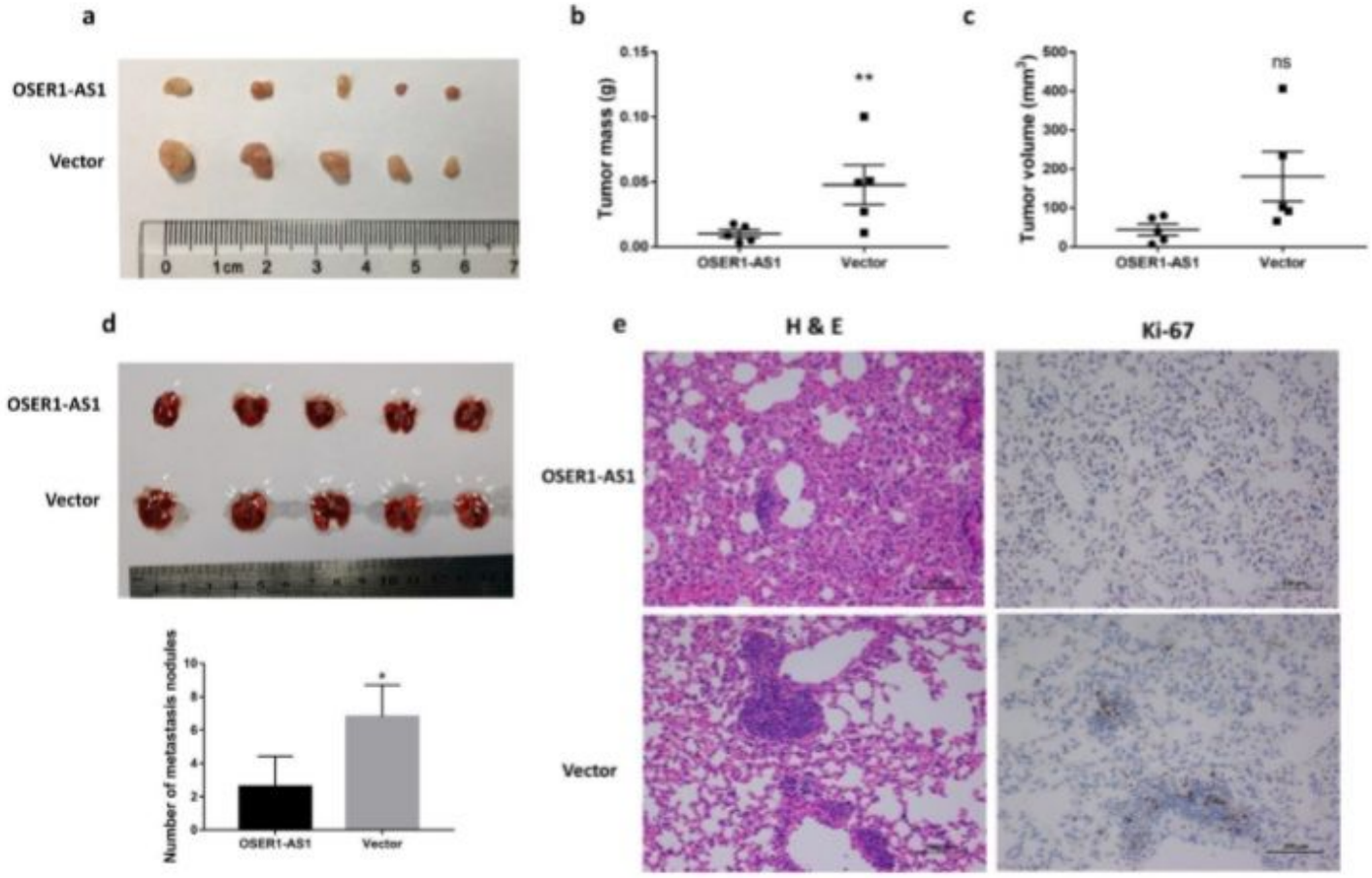


## Figure 3

Overexpression of OSER1-AS1 inhibits lung cancer cell growth and metastasis in vivo. (a) Tumors from the OSER1-AS1 and vector control groups upon resection from BALB/c-nude mice five weeks after subcutaneously injected with stable transfected A549 cells (5.0 × 106) into the left flanks. (b) Tumor weight from the OSER1-AS1 and vector control groups. Lines represent the mean and SEM of five independent experiments. ** OSER1-AS1 vs. vector control, Mann-Whitney U-test, $P < 0.01$. (c) The tumor volume was calculated using the equation $V = 0.5 \times D \times d2$ (V, volume; D, longitudinal diameter; d, latitudinal diameter). Lines represent the mean and SEM of five independent experiments. ns OSER1-AS1 vs. vector control, Mann-Whitney U-test, $P > 0.05$; (d) Lungs from nude mice in each group 5 weeks after injections of stable transfected A549 cells (1.0 × 106). Top panel: Arrows point to tumor nodules on the lung surface. Bottom panel: the numbers of lung metastatic nodules on lung surfaces were counted. *OSER1-AS1 vs. vector control, Mann-Whitney U-test, $P < 0.05$. (e) Left panels: H&E staining of lung tissue slices showed that more metastatic nodules were present in vector control group than OSER1-AS1 overexpression group. Magnification, ×200; Right panels: immunohistochemical analysis of proliferation marker Ki-67 showed that Ki-67 expression levels were significantly lower in OSER1-AS1 overexpression group than those in control vector group.

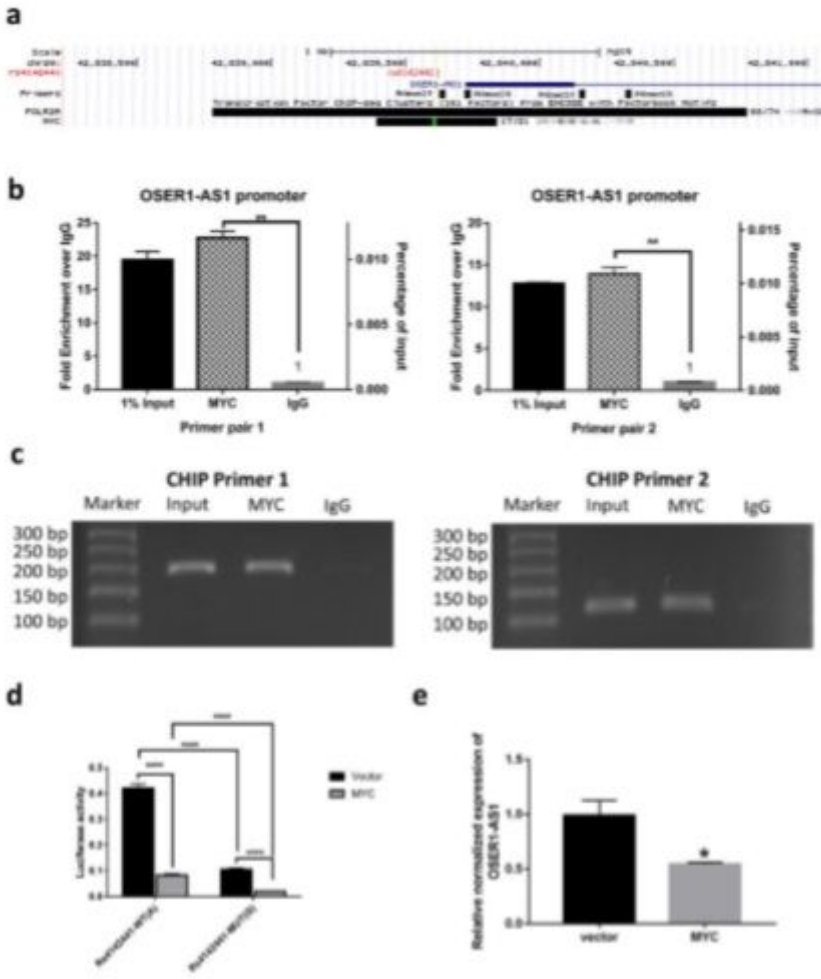


## Figure 4

MYC directly binds to the promoter region of lncRNA OSER1-AS1. (a) The UCSC genome browser representation of the genomic organization of the promoter region of OSER1-AS1 gene in human chromosome (hg19, chr20:42839726-42854667), where exons are indicated by solid blue boxes and introns by the blue line. Rs4142441 is represented as a vertical red bar. The Primer track shows the binding position of two pairs of primers that were used to detect the promoter sequence of OSER1-AS1. F primer, forward primer; R primer, reverse primer. The Transcription Factor ChIP-seq Clusters track shows regions of transcription factor binding derived from a large collection of ChIP-seq experiments performed by the ENCODE project. The POLR2A box represents the peak cluster of transcription factor occupancy of RNA polymerase II subunit A, whereas the MYC box represents the peak cluster of transcription factor occupancy of MYC, with the darkness of the box being proportional to the maximum signal strength observed in any cell line contributing to the cluster. (b) ChIP-PCR assays were performed to detect whether MYC directly bound to the promoter of OSER1-AS1. Left panel: primer pair 1. Right panel: primer pair 2. Error bars represent the SD of three independent experiments. Two-tailed Student's t-test: **, P < 0.01. (c) qRT-PCR products of the promoter region of OSER1-AS1. qRT-PCR wasconducted after ChIP, using two pairs of primers. DNA fragments pull-down by IgG antibody was used as a negative control. (d) Luciferase assays of H1299 cells co-transfected with pGL3-basic-OSER1-AS1 reporter with rs4142441-

WT(A) or rs4142441-MUT(G)promoter sequence and MYC overexpression vectors or control vector. (e) The qRT-PCR analysis of relative OSER1-AS1 expression

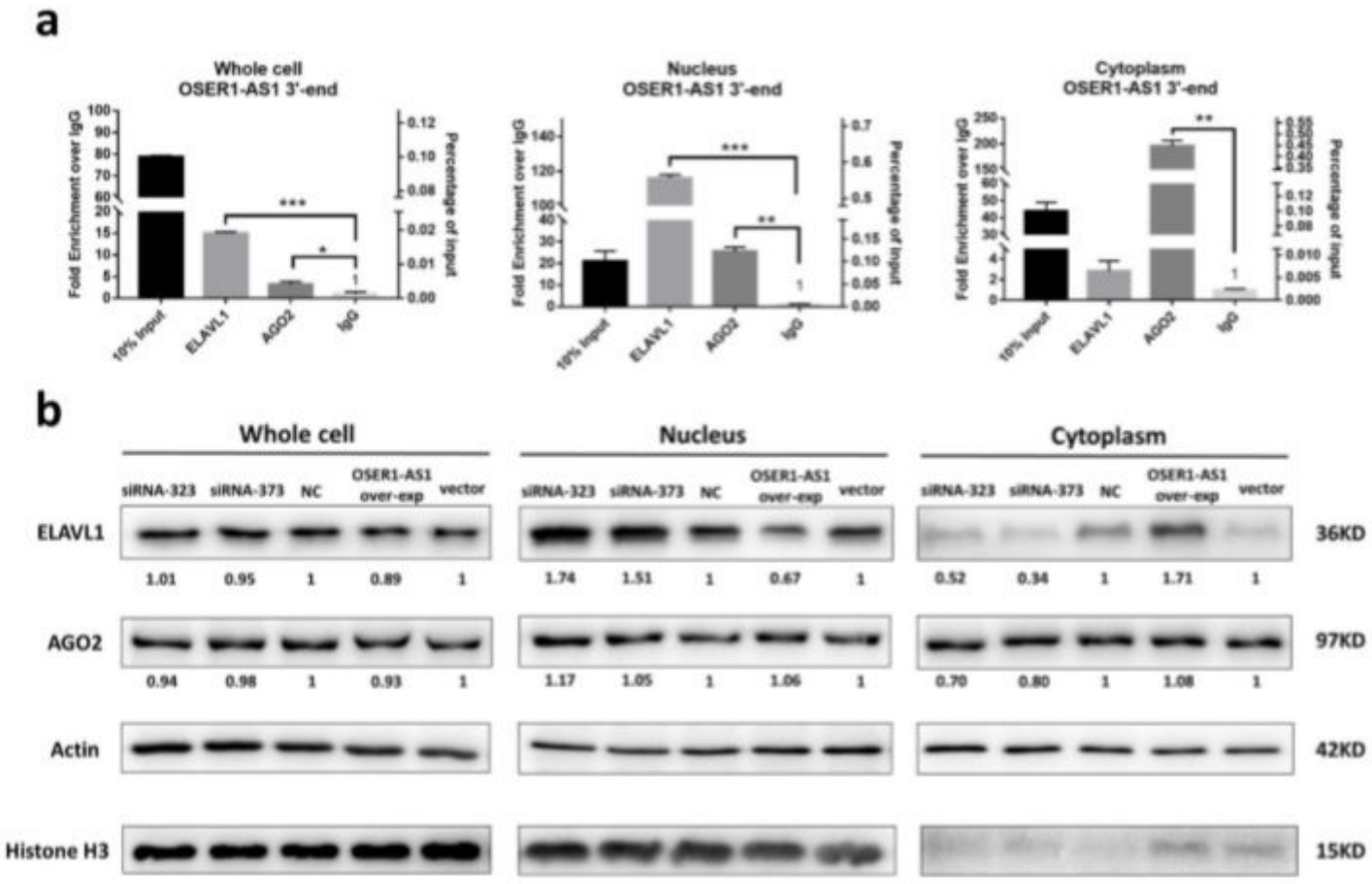


## Figure 5

LnRNA-protein interaction between OSER1-AS1 and ELAVL1. (a) RNA immunoprecipitation (RIP) was performed in H1299 cells using either control IgG, anti-ELAVL1 or anti-AGO2 antibodies. Immunoprecipitated OSER1-AS1 RNA was quantified by qRT-PCR. The relative abundance of RNA-protein complex in cell lysate was expressed as either the fold enrichment normalized to the control IgG (Left Y-axis) or percentage of input (Right Y-axis). Error bars represent the SD of three independent experiments. Two-tailed Student's t-test: *, P < 0.05; **, P < 0.01; ***, P < 0.001. (b) The protein expression levels of ELAVL1 and AGO2 in H1299 cells were detected by western blot after knockdown and overexpression of OSER1-AS1. Cell lysates were collected for western blotting 48 hr post-transfection. The numbers below the bands indicated the fold change of quantitative analysis results. Beta-actin was used as positive controls for whole cell and cytoplasmic. Histone H3 was used as positive controls for nucleus lysate.

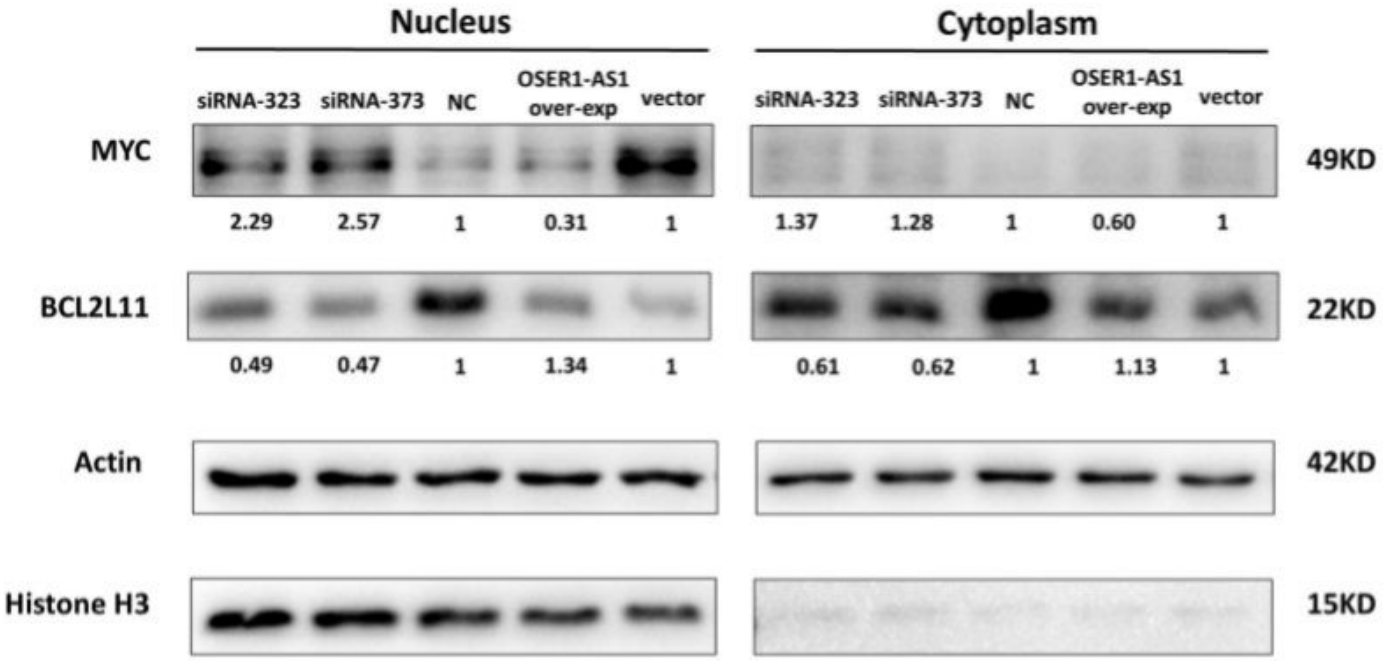


## Figure 6

The protein levels of MYC and BCL2L11 in H1299 cells were detected by western blot after knockdown and overexpression of OSER1-AS1. The protein expression levels of MYC and BCL2L11 in H1299 cells were detected by western blot after knockdown and overexpression of OSER1-AS1. Cell lysates were collected for western blotting 48 hr post-transfection. The numbers below the bands indicate the fold change of quantitative analysis results. Beta-actin was used as positive controls for whole cell and cytoplasmic. Histone H3 was used as positive controls for nucleus lysate.

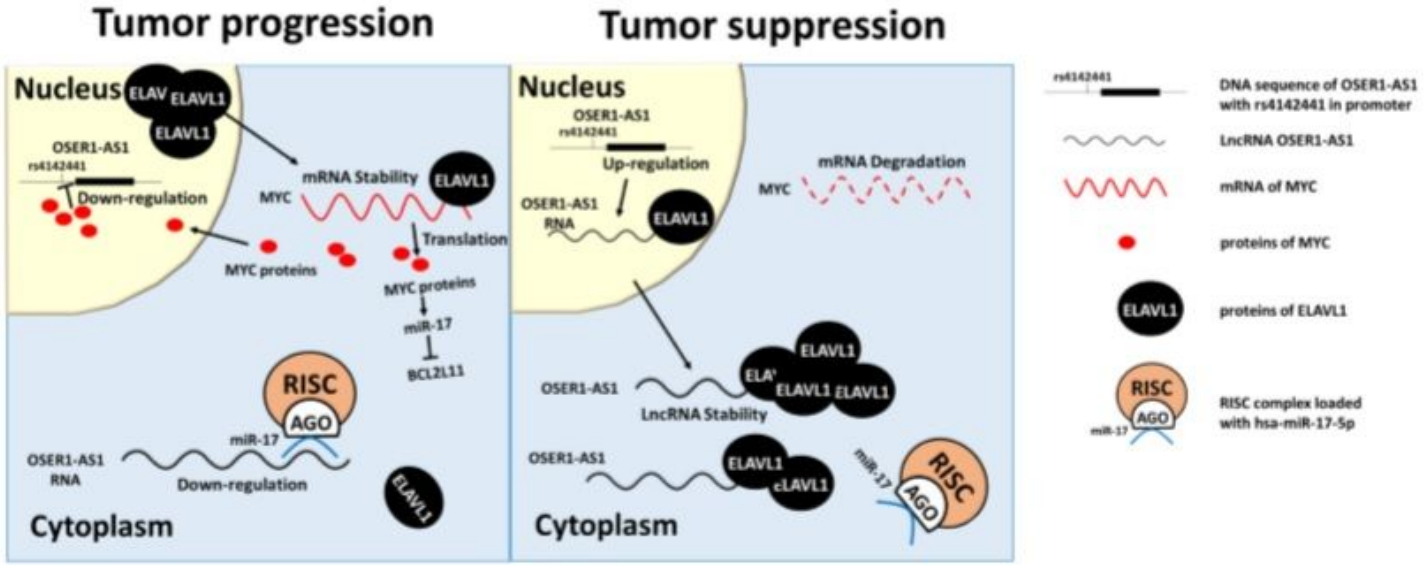


## Figure 7

A proposed model depicting the potential mechanisms of OSER1-AS1 as a tumor suppressor lncRNA in NSCLC. Left panel: in a scenario of tumor progression, OSER1-AS1 is suppressed by transcription factor MYC in the nucleus and inhibited by miR-17-5p in the cytoplasm. ELAVL1 are transported from the nucleus to the cytoplasm to stabilize mRNAs of MYC and increases its translational efficiency. The MYC proteins in turn down-regulate OSER1-AS1 and BCL2L11, and up-regulate miR-17-5p. Right panel: in a scenario of tumor suppression, the cytoplasmic level of OSER1-AS1 increases to a level to be able to overcome the inhibitory effect of miR-17-5p. Free cytoplasmic OSER1-AS1 forms RBP-RNA complexes with ELAVL1 to sequester it from its target MYC mRNAs and possibly other oncogenic genes regulated by ELAVL1.

## Supplementary Files

This is a list of supplementary files associated with this preprint. Click to download.

- SupplementaryTables20200425.pdf
- SupplementaryFigures.pdf
- SupplementaryMethods.pdf